Acta Pharmaceutica Sinica B 2021;11(10):3120–3133

Chinese Pharmaceutical Association
Institute of Materia Medica, Chinese Academy of Medical Sciences

Acta Pharmaceutica Sinica B

www.elsevier.com/locate/apsb
www.sciencedirect.com

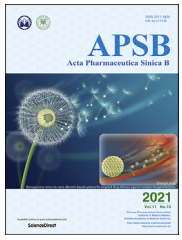

ORIGINAL ARTICLE

PD0325901, an ERK inhibitor, enhances the efficacy of PD-1 inhibitor in non-small cell lung carcinoma

Min Luo[a,†], Yuhui Xia[a,†], Fang Wang[a], Hong Zhang[a], Danting Su[a], Chaoyue Su[a,b], Chuan Yang[a], Shaocong Wu[a], Sainan An[a], Suxia Lin[a,*], Liwu Fu[a,*]

[a]*State Key Laboratory of Oncology in South China, Collaborative Innovation Center for Cancer Medicine, Guangdong Esophageal Cancer Institute, Sun Yat-sen University Cancer Center, Guangzhou 510060, China*
[b]*Pharmacy College, Guangzhou Medical University, Guangzhou 510182, China*

Received 3 January 2021; received in revised form 3 February 2021; accepted 10 February 2021

KEY WORDS

ERK1/2;
PD-L1;
PD-1;
PD0325901;
NSCLC;
Immunotherapy;
Targeted therapy;
Combination therapy

Abstract ERK pathway regulated the programmed death ligand-1 (PD-L1) expression which was linked to the response of programmed death-1 (PD-1)/PD-L1 blockade therapy. So it is deducible that ERK inhibitor could enhance the efficacy of PD-1 inhibitor in cancer immunotherapy. In this study, PD0325901, an oral potent ERK inhibitor, strongly enhanced the efficacy of PD-1 antibody *in vitro* and *in vivo* models in non-small cell lung carcinoma (NSCLC) cells. Mechanistically, PD0325901 or shRNA-*ERK1/2* significantly downregulated the PD-L1 expression in NSCLC cells and increased the $CD3^+$ T cells infiltration and functions in tumor tissue. There was a positive correlation between the p-ERK1/2 expression and PD-L1 expression in patients with NSCLC. And the patients with low p-ERK1/2 expression were observed a high response rate of PD-1/PD-L1 blockage therapy. Our results demonstrate that PD0325901, an ERK inhibitor, can enhance the efficacy of PD-1 blockage against NSCLC *in vitro* and *in vivo* models. And the combination of ERK inhibitor such as PD0325901 and PD-1/PD-L1 blockage is a promising regimen and encouraged to be further confirmed in the treatment of patients with NSCLC.

*Corresponding authors. Tel.: +86 20 873431-63, fax: +86 20 87343170.
E-mail addresses: linsx@sysucc.org.cn (Suxia Lin), Fulw@mail.sysu.edu.cn (Liwu Fu).
†These authors made equal contributions to this study.

Peer review under responsibility of Chinese Pharmaceutical Association and Institute of Materia Medica, Chinese Academy of Medical Sciences.

https://doi.org/10.1016/j.apsb.2021.03.010

1. Introduction

Lung cancer is the leading cause of cancer-related mortality globally[1], with around 80%−85% of cases are non-small cell lung carcinoma (NSCLC)[2]. And nearly 70% of lung cancer patients are diagnosed with advanced or metastatic disease which have poor prognosis[1,3]. Because of the limited surgical options and low response rate (only 15%−30%) of chemotherapy, the 5-year survival of patients with advanced NSCLC is only 15%[3−5]. Recently, there have been great breakthroughs in immunotherapy, particularly the immune checkpoint programmed death-1(PD-1)/programmed death ligand-1 (PD-L1) blockade for various cancer types. Several immunotherapeutic agents such as monoclonal antibodies (mAbs) targeting PD-1 (nivolumab and pembrolizumab) and PD-L1 (atezolizumab) have been approved by U.S. Food and Drug Administration (FDA)[6,7], and have provided an alternative option for patients with NSCLC in the second-line treatments[8].

PD-1 is expressed on activated T cells, and PD-L1 is typically expressed on antigen-presenting cells (APCs) and several cancer cell types including NSCLC[9]. PD-L1 overexpression is very common in various malignancies[10], and correlates with unfavorable prognosis and lower survival rates[11]. The interaction between PD-1 and PD-L1 induces activated T cell apoptosis or exhaustion, thus inhibiting the activity of anti-tumor immunity[12]. Inhibition of the PD-1/PD-L1 axis could restore the activity of T cells[13]. Expression of PD-L1 on tumor cells is regulated by intrinsic and extrinsic mechanisms. The intrinsic PD-L1 expression is driven by oncogenic activation, and the extrinsic PD-L1 expression is induced by IFN-γ secreted from tumor infiltrating lymphocytes (TILs)[14]. PD-1/PD-L1 immune checkpoint blockade can induce long-term durable responses in cancer patients. However, only a minority (less than 20%) of patients get benefits from PD-1/PD-L1 blockage in patients with NSCLC[7]. So it is conceivable that one of the promising approaches to improve the efficacy of these therapies is combination therapy. To this point, there are amounts of clinical trials currently testing the efficacy of combination therapy of PD-1/PD-L1 antibody and conventional chemotherapy or targeted therapy or other immune molecules such as cytotoxic T lymphocyte associated protein 4 (CTLA-4), T-cell immunoglobulin mucin 3 (TIM-3), lymphocyte-activation gene 3 (LAG3), tumor necrosis factor receptor superfamily, member 4 blockage[15−19]. A lot of kinase inhibitors such as EGFR, ALK, c-MET, MEK, ERK and so on were used to treat NSCLC patients with oncogenic alterations[20−22]. Although targeted therapies dramatically improve patients' survivals, invariably acquired resistance mutations or activated compensatory pathways triggered targeted drug resistance and limited successful cancer therapy[23]. On the other hand, NSCLC cells bearing *EGFR*, *KRAS*, *BRAF*, *ALK* or *RET* mutations were found with high level of PD-L1 expression which was associated with the activation of MEK/ERK or PI3K/AKT/mTOR pathway[24−27]. Patients with driver gene mutations like *ALK* or *EGFR* benefit much less from PD-1 or PD-L1 inhibitor therapy due to a lack of an inflammatory microenvironment[28]. So the inhibition of molecules regulating PD-L1 expression may be a potential combination agent with PD-1/PD-L1 blockade. Treatment with MAPK or BRAF inhibitors enhances the expression of melanoma antigens and induces a more favorable tumor microenvironment, as evidenced by the decreases of the immunosuppressive cytokines[29] and an increase of $CD8^+$ T cells infiltration[30], giving the support for potential synergy of targeted therapy and immunotherapy. An increasing evidence suggests that targeted therapy modulates the tumor immune microenvironment such as T cells infiltration which would optimize tumor cells to the antitumor activity of immunotherapy and then increases the percentages of patients benefiting from PD-1/PD-L1 inhibitors[31,32]. There are some combination therapies of mTOR inhibitor and PD-1/PD-L1 antibody going on clinical trial in solid tumors, such as sirolimus+durvalumab for NSCLC (NCT04348292), nivolumab+nab-rapamycin for advanced sarcoma (NCT03190174).

The MAPK/ERK pathway has been identified as a common dysregulated pathway in several cancers, most notably was in NSCLC. MEK/ERK has well-established roles in the regulation of a large variety of processes of tumorigenesis[33,34]. ERK1/2, which is ubiquitously expressed in mammalian tissues and cell types, is generally activated by extracellular stimuli, including a range of growth factors and cellular stresses[33,34]. Accumulating evidences in preclinical models indicate the benefits of using MEK/ERK1/2 inhibitory strategies for the treatment of human cancers[35]. PD0325901, an oral potent small-molecule inhibitor of MEK/ERK signaling, was observed anti-proliferative and antitumor activity in preclinical models of cancer and go on phase II clinical trial[36,37]. There are 3 ongoing phase II clinical trials (NCT02022982, NCT02039336, and NCT00174369) testing the effects of PD0325901 on tumor growth inhibition in patients with NSCLC[35]. Herein, we have launched the hypothesis that the ERK inhibitor PD0325901 enhances the efficacy of PD-1 blockage *via* down-regulating PD-L1 expression in NSCLC.

2. Materials and methods

2.1. Cells and cell culture

The NSCLC cells (H1299, H460, A549, PC-9, SPCA1, GLC-82 and H1975), Lewis lung cancer (LLC) cells and 293T cells were obtained from ATCC and were validated by short-tandem-repeat (STR) analysis (except for LLC cells). All cells were maintained in Dulbecco's modified Eagle's medium (DMEM) supplemented with 10% fetal bovine serum. Peripheral blood mononuclear cells (PBMCs) were cultured in the presence of 100 IU/mL human IL-2. All cells were cultured in a humidified incubator at 37 °C containing 5% CO_2.

2.2. Chemicals and reagents

PD0325901 and PD-1 blocking antibody (pembrolizumab) were purchased from Selleck Chemicals. Anti-PD-L1, anti-phospho ERK1/2 and anti-ERK1/2 antibodies were obtained from Santa Cruz Biotechnology. The antibody against GAPDH was purchased from Proteintech. The anti-mouse CD3 and granzyme B antibodies for immunohistochemistry were purchased from Abcam. The anti-human PD-L1 and p-ERK1/2 for immunohistochemistry were obtained from Santa Cruz Biotechnology. The anti-human CD3 and CD8 antibodies for immunohistochemistry were purchased from Zsbio. Dimethyl sulfoxide and 3-(4,5-dimethylthiazol-yl)-2,5-diphenyltetrazolium bromide (MTT) were products of Sigma−Aldrich. DMEM and fetal bovine serum were products of Gibco. Penicillin, streptomycin and trypsin were obtained from Thermo Fisher Scientific. InVivoMab anti-mouse PD-1 (CD279) was purchased from BioXcell.

2.3. MTT assay

The MTT assay was performed according to previous report[38]. NSCLC cells were harvested during logarithmic growth phase and plated at 2500−3000 cells/well in 96-well plates in a final volume of 190 μL/well. After plating for 24 h, the cells were treated with 10 μL of PD0325901 at concentrations ranging from 0 to 1 mmol/L for another 68 h at 37 °C. Then, 20 μL MTT at 5 mg/mL was added to each well and incubated for another 4 h. The supernatant was then removed, followed by the addition of 150 μL of DMSO to dissolve the MTT crystals. The absorbance at 540 nm/655 nm dual wavelengths was assessed using a Model 550 Microplate Reader (Bio-Rad). The concentration of PD0325901 suppressing cell proliferation by 20%, calculated from survival curves using the Bliss method, was selected for further experiments. All experiments were repeated at least three times, and the mean value ± standard deviation (SD) was calculated.

2.4. Western blotting analysis

As previous report described[39], briefly, the whole-cell extracts were collected and lysed with RIPPA Lysis Buffer (Beyotime). Cell lysates were quantified with Pierce BCA Protein Assay Kit (Thermo Fisher Scientific) according to manufacturer's instructions. The proteins were separated *via* SDS-polyacrylamide electrophoresis on an 8% gel and transferred onto PVDF membranes (Millipore). After blocking with 5% fat-free milk for 1 h, membranes were probed with specific primary antibodies and HRP-conjugated goat anti-rabbit or anti-mouse secondary antibodies. The Clarity™ Western ECL Substrate (Bio-Rad) was used to visualize protein bands.

2.5. Real-time PCR analysis

The real-time PCR analysis was conducted as previously described[40]. In brief, the total cellular RNA was isolated by Trizol Reagent (Thermo Fisher Scientific) according to the manufacturer's protocols. The qPCR primers were as follows: *PD-L1*, forward: TATGGTGGTGCCGACTACAA, reverse: TGCTTGTCCAGATGACTTCG; β-actin, forward: TCCTGTGGCATCCACGAAACT, reverse: GAAGCATTTGCGGTGGACGA. The qPCR reactions were conducted using ChamQ SYBR qPCR Master Mix (without ROX) (Vazyme) following the manufacturer's protocols. Data were analyzed using the $2^{-\Delta\Delta Ct}$ method after normalization with the β-actin expression level in each sample.

2.6. Immunohistochemistry

The clinical tumor specimens were collected from patients who were diagnosed with NSCLC in Sun Yat-sen University Cancer Center, Guangzhou, China. For patient specimens, all patients were consented and enrolled to Sun Yat-sen University Cancer Center IRB approved protocols, in accordance with ethical guidelines, allowing the collection and analysis of clinical data, archival and paraffin specimens (No. YB2020-008-01). This study conforms to the Declaration of Helsinki. Tumor samples were fixed in formalin and embedded in paraffin according to standard laboratory pathology practice, and stored at the department of pathology at the Sun Yat-sen University Cancer Center. For patients' specimens, the paraffin sections were incubated with primary anti-human antibodies at different dilutions (PD-L1, 1:100, p-ERK1/2, 1:200, CD3, 1:100, CD8, 1:200) for 50 min at 37 °C, and incubated with secondary antibodies. Mice tumors were harvested, fixed in 10% buffered formalin overnight, and embedded in paraffin before being cut into 4 μm sections. All paraffin sections were incubated with primary anti-mouse antibodies (CD3, 1:100, granzyme B, 1:100) for 50 min at 37 °C, and incubated with secondary antibodies. The staining was detected by exposure to DAB Kit (Zisbio) according to the manufacturer's instructions. Slides were stained with hematoxylin for 6 min and the staining was quantified using at least 5 randomly selected 200× or 400× fields of view. The protein expression was independently assessed by two pathologists. PD-L1 expression was considered positive if at least 5% of the tumor cells exhibited membranous PD-L1 staining[41].

2.7. Establishment of ERK1/2-knockdown cells

The transfection was performed according to previous methodology[39]. The shRNA vectors for *ERK1* or *ERK2* shRNAs and a negative shRNA control (shctrl) vector were transiently transfected using a pSIH-H1-puro Lentivector Packaging Kit (System Biosciences). The sequences of shRNAs were as follows, shRNA control (shctrl): CAACAAGATGAAGAGCACCAA; *ERK1* sh1: GCAGCTGAGCAATGACCATAT, sh2: GCTGAACTCCAAGGGCTATAC. The NSCLC cells infected with *ERK1* shRNAs were presented as *ERK1*sh1 and *ERK1*sh2, respectively. *ERK2*sh1: GGACCTCATGGAAACAGATCT, sh2: GCTGCATTCTGGCAGAAATGC. The NSCLC cells infected with *ERK2* shRNAs were presented as *ERK2*sh1 and *ERK1*sh2, respectively. The 293T cells were transfected with Lipofectamine 2000 Reagent (Thermo Fisher Scientific) according to the manufacturer's instructions. H460 and H1299 cells were infected and incubated with the viral particles overnight at 37 °C. After 48 h, cells were screened under puromycin selection (3 μg/mL for H460 cells, and 4 μg/mL for H1299 cells).

2.8. In vivo experiments

All animal studies were performed with the permission of the institutional committee of Sun Yat-sen University Cancer Center, in compliance with protocols approved by the Guangdong Provincial Animal Care and Use Committee and experimental guidelines of the Animal Experimentation Ethics Committee of Sun Yat-sen University Cancer Center (No. L102012020120A). The 4−6-week-old NSG mice were obtained from Sibeifu (Beijing) Laboratory Animal Technology. LLC cells (1×10^6 cells/mouse) were suspended in 100 μL PBS and subcutaneously injected into the flank of NSG mice. About 9 days later, the tumors reached about 50−100 mm^3, tumor-bearing mice were randomized into two groups: control and PD0325901 group. The animals in control group were treated with saline and PD0325901 was administered orally at a dose of 20 mg/kg every other day. We obtained immunocompetent C57BL/6J mice from the Laboratory Animal Unit of the Guangdong Province. LLC cells (2×10^5 cells/mouse) were suspended in 100 μL PBS and

subcutaneously injected into the flank of 4−6-week-old female C57BL/6J mice as previously described[42]. About 11 days later, the tumors reached about 50−100 mm^3, tumor-bearing mice were randomized into four groups: control, PD-1 antibody, PD0325901, and PD0325901+PD-1 antibody. The animals in control group were treated with saline and InVivoMAb rat IgG2a isotype control (10 mg/kg, BioXCell). PD0325901 was administered orally at a dose of 20 mg/kg every other day; PD-1 antibody was administered every 4 days intraperitoneally (10 mg/kg) until the end of the study. During the treatment period, tumor volumes were recorded every other day using a digital caliper measurement of two diameters of the tumor (length and width). Tumor volumes were calculated according to Eq. (1):

$$\text{Volume } (mm^3) = \text{Length } (mm) \times \text{Width } (mm)^2 \times 0.5 \quad (1)$$

Body weights were assessed every other day using a weight scale and recorded in grams. Mice were euthanized when tumor volumes >2000 mm^3. According to previous studies[43,44], death is defined as the tumor volume reached 1000 mm^3 and the survival curve was plotted. Tumors tissues excised from mice were fixed with formalin for further histopathology analysis.

2.9. Flow cytometry analysis

As previously reported[38], 2.5×10^5 cells were plated per well in a 6-well plate. The cells were treated with 1 μmo/L PD0325901 for 48 h, and then collected, pelleted, and resuspended in PBS. Cells were stained with anti-human PD-L1 (Biolegend) and analyzed by flow cytometry. As for the HLA-match analysis, the tumor cells and PBMCs were stained with anti-human HLA-A2 (Biolegend) and analyzed by flow cytometry as previously reported[45,46]. The Flowjo (Treestar) software was used for the analysis of flow cytometry data. The standardized fluorescence intensities were calculated by dividing the median fluorescence intensities of specific antibodies by the median fluorescence intensities of isotype controls. The results are presented as mean ± SD of three independent experiments.

2.10. In vitro co-culture systems

Fresh PBMCs were isolated from healthy donors. Based on the co-culture system reported previously[42], we stimulated PBMCs with anti-CD3e (3 μg/mL) (BioLegend) for 4 h before being plated at 1×10^5 cells/well. Isolated PBMCs were subsequently co-cultured with NSCLC cells at a ratio of 4:1. To block the binding of PD-1 with PD-L1, PD-1 blocking antibody (pembrolizumab, 100 μg/mL) was used. After 3−4 days of co-incubation, the PBMCs were discarded and the remaining tumor cells were stained with Gimesa (Sigma−Aldrich). And the relative intensity was measured by Image J software. The levels of TNF-α, IFN-γ, IL-6 in co-culture medium were measured by ELISA assay with the manufacturer's instructions.

2.11. Statistical analysis

Statistical analysis was carried out using SPSS Statistics 19 software (IBM) using Student's *t*-test or one-way ANOVA analysis. Experiments were repeated in triplicate. Data are expressed as mean ± SD. *P* values for survival curves are assessed by log-rank test. Statistical significance is defined as $P < 0.05$.

3. Results

3.1. The cytotoxicity of PD0325901 on NSCLC cells and PBMCs

We examined the cytotoxicity of PD0325901 on different NSCLC cells and PBMCs by MTT assay. As shown in Fig. 1A, more than 80% of tumor cells and PBMCs survived when treated with PD0325901 under the concentration of 1.0 μmol/L. We chose 1.0 μmol/L as working concentration for further study in combination therapy.

3.2. PD0325901 enhanced the efficacy of PD-1 antibody in vitro

To explore the effect of PD0325901 on antitumor immunity activity, we firstly detected the HLA-A2 type of the tumor cells and PBMCs (Fig. 1B). All the cells used in the co-culture system were HLA-A2 type matched. The NSCLC cells were pre-treated with PD0325901 or PBS for 48 h. Then we co-cultured the tumor cells with the PBMCs at different ratios. H460 cells or A549 cells with PD0325901 pretreatment were observed more cancer cells lysis in co-culture with PBMCs than that with PBS pretreatment, and with the co-cultured PBMCs number increased, the cancer cells lysis increased (Fig. 1C and D). To further investigate the effect of the combination of PD-1 antibody (PD-1 Ab) and PD0325901 on cancer cell lysis in the co-culture system, cancer cell lysis was examined. The results show that the survival rates of H460 cells in each group were 72.40 ± 0.58% of those in control group, 44.47 ± 1.57% in PD0325901, 72.52 ± 0.68% in PD-1 Ab, 36.94 ± 1.03% in PD0325901+PD-1 Ab (Fig. 1E). In A549 cells, the survival rates of tumor cells in each group were 52.08 ± 2.66% of those in control group, 41.43 ± 3.37% in PD0325901 group, 52.28 ± 4.54% in PD-1 Ab, 28.49 ± 3.16% in PD0325901+PD-1 Ab group, respectively (Fig. 1F). The results show the combination treatment kills more cancer cells than either PD-1 antibody pembrolizumab or PD0325901 alone.

3.3. PBMCs exhibited an enhancement of cancer cell lysis by PD-1 antibody in co-culture with ERK1/2-knockdown NSCLC cells

In order to explore the effect of ERK1/2 inhibition on antitumor immunity activity, the NSCLC cells were transfected with shRNAs targeting *ERK1* or *ERK2* respectively. Then the PBMCs were co-cultured with the *ERK1*- or *ERK2*-knockdown cells in the presence of PD-1 antibody, respectively. The tumor cells and PBMCs were HLA-A2 matched (Fig. 1A). The results show that the survival rates of H460 cells were, control 67.97 ± 0.23%, PD-1 Ab 66.33 ± 2.17%, *ERK2*sh1 50.84 ± 1.58%, *ERK2*sh1+PD-1 Ab 25.19 ± 3.77%, respectively (Fig. 1G). The survival rates of H1299 cells were, control 51.00 ± 0.43%, PD-1 Ab 48.43 ± 1.03%, *ERK2*sh1 38.94 ± 0.90%, *ERK2*sh1+PD-1 Ab 23.89 ± 0.86%, respectively (Fig. 1H). When knocking-down *ERK1*, the survival

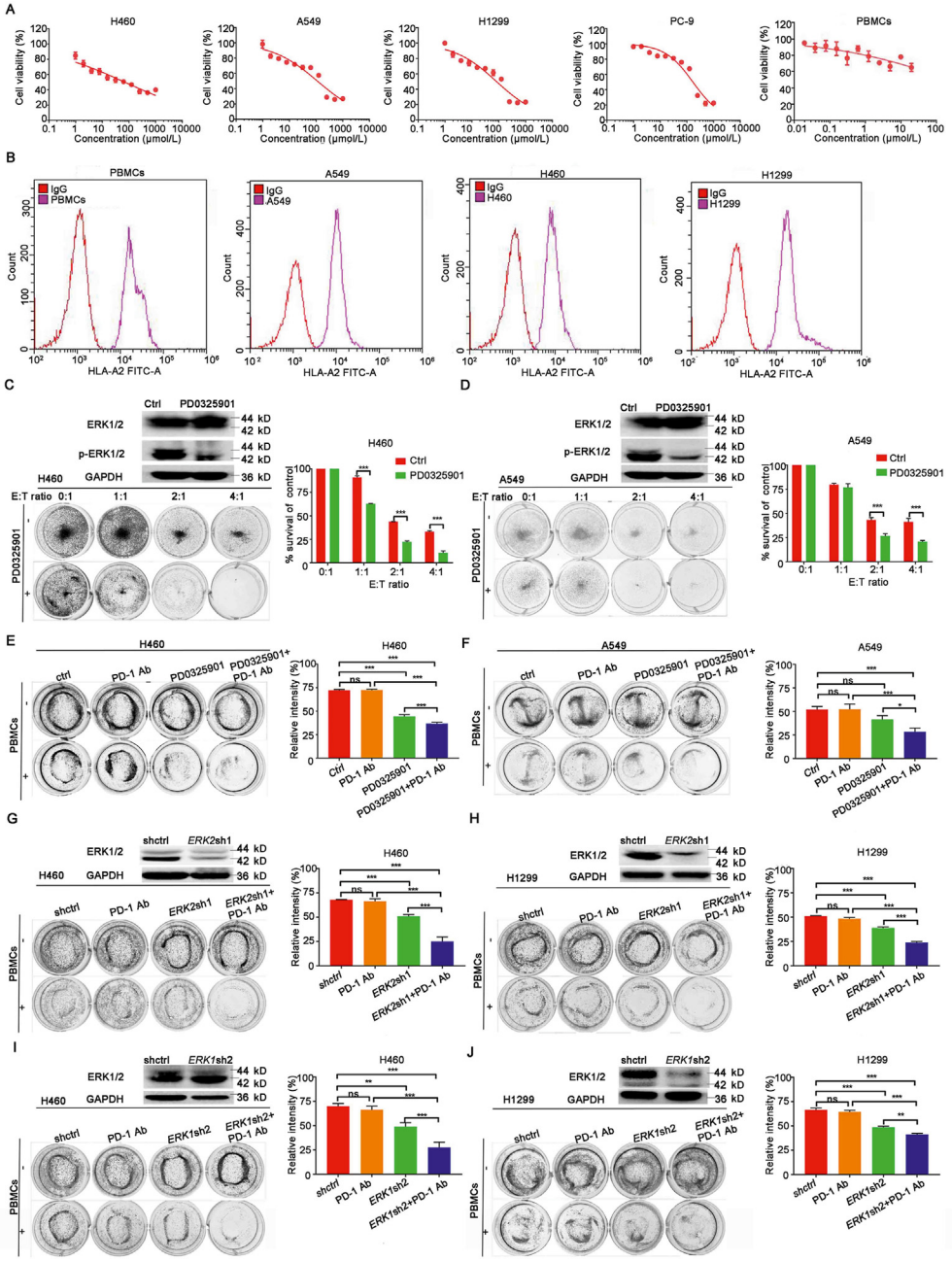

Figure 1 PD0325901 enhanced the efficacy of PD-1 antibody *in vitro*. (A) The MTT assay of NSCLC cells and PBMCs treated with different concentrations of PD0325901. Results are presented as mean ± SD and the experiment was performed in triplicate. (B) The flow cytometry analysis of HLA-A2 expression of tumor cells and PBMCs. (C) and (D) The H460 cells or A549 cells were pretreated with PD0325901 (1 μmol/L) or PBS for 48 h and then co-cultured with PBMCs at different ratios in 12-well plates for 4 days. The surviving tumor cells were visualized by Giemsa staining. The relative intensity was measured by Image J software. E:T ratio, effector cells (PBMCs):target cells (tumor cells) ratio. (E) and (F) The PBMCs-mediated tumor cell killing assay of PD0325901-pretreated (1 μmol/L, 48 h) H460 cells or A549 cells in the presence of PD-1 antibody pembrolizumab (100 μg/mL). (G) and (H) The PBMCs-mediated tumor cell killing assay of *ERK2*-knockdown H460 cells or H1299 cells in the presence of PD-1 antibody pembrolizumab (100 μg/mL). (I) and (J) The PBMCs-mediated tumor cell killing assay of *ERK1*-knockdown H460 cells or H1299 cells in the presence of PD-1 antibody pembrolizumab (100 μg/mL). All the results are presented as mean ± SD and the experiment was performed in triplicate; $^{*}P < 0.05$, $^{**}P < 0.01$, $^{***}P < 0.001$, ns, no significance.

rates of H460 cells were control 69.95 ± 6.30%, PD-1 Ab 66.35 ± 3.01%, *ERK1*sh2 48.96 ± 3.36%, *ERK1*sh2+PD-1 Ab 27.66 ± 4.40%, respectively (Fig. 1I). The survival rates of H1299 cells were control 66.52 ± 1.62%, PD-1 Ab 64.53 ± 1.26%, *ERK1*sh2 48.64 ± 0.88%, *ERK1*sh2+PD-1 Ab 41.32 ± 0.89%, respectively (Fig. 1J). As the results show, the cell lysis was significantly increased compared to negative control when *ERK1* or *ERK2* was downregulated. The administration of PD-1 antibody notably enhanced the PBMCs mediated cells death in both *ERK1*- and *ERK2*-knockdown cells, and there was no difference between

ERK1 and *ERK2* depletion in cancer cell death in combination with PD-1 Ab.

3.4. *PD0325901 potentiated the efficacy of PD-1 antibody on the inhibition of tumor growth in vivo*

To further investigate the enhancement of PD-1 antibody by PD0325901, we firstly established a small animal model in NSG mice. The LLC cells were subcutaneously injected into NSG mice and treated with saline or PD0325901 (20 mg/kg) every other day, respectively. At the end of the experiment, there was no significant difference in tumor growth (Fig. 2A−C) and tumor weight (Fig. 2D) between the control group and PD0325901 group, suggesting that there were no cell-autonomous effects of ERK inhibition induced tumor growth inhibition at the dose we chose. Then the models of the immunocompetent C57BL/6J mice bearing Lewis lung cancer cells were established. The mice were treated with saline, PD0325901, anti-mouse-PD-1 antibody, PD0325901+anti-mouse-PD-1 antibody, respectively. At the end of the experiment, the tumor volume of each group was control 2522.12 ± 405.18 mm^3, PD-1 Ab 1512.85 ± 498.24 mm^3, PD0325901 839.15 ± 317.65 mm^3, PD0325901+PD-1 Ab 249.06 ± 82.31 mm^3, respectively (Fig. 2E−G). The combination group significantly inhibited the tumor growth and the tumor volume was significantly decreased compared with single drug group (PD0325901+PD-1 Ab *vs*. PD0325901, $P < 0.05$, PD0325901+PD-1 Ab *vs*. PD-1 Ab, $P < 0.001$, Fig. 2F and G). A significant survival advantage was observed in mice treated with the combination therapy compared to control or monotherapy (Fig. 2H). Importantly, no animal death or body weight loss was observed in the duration of treatments (Fig. 2I).

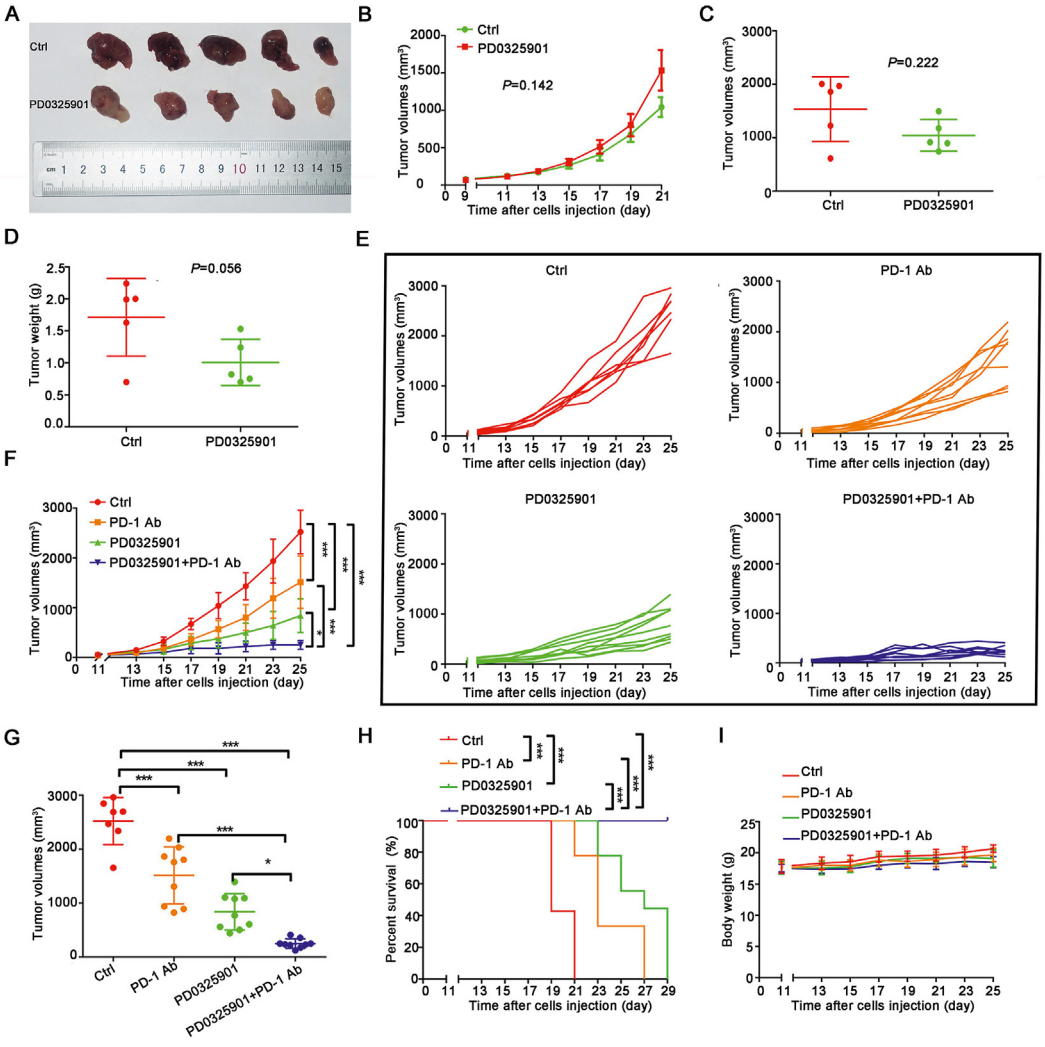

Figure 2 PD0325901 enhanced the efficacy of PD-1 antibody *in vivo*. (A) The image of tumor samples of NSG mice upon two treatments. (B) The tumor volumes curve of the NSG mice with two treatments. (C) and (D) The tumor volumes and tumor weights of NSG mice at the endpoint of the experiment. (E) and (F) The tumor volume curves of the C57BL/6 mice with different treatments. (G) The tumor volumes of all mice at the endpoint of the experiment. All the results are presented as mean ± SD and the experiment was performed in triplicate; *$P < 0.05$, **$P < 0.01$, ***$P < 0.001$, ns, no significance. (H) The Kaplan−Meier survival curves across treatment groups in mice. (I) The body weight changes of the mice in four treatment groups.

3.5. *PD0325901 increased lymphocytes infiltration and function*

To investigate the effect of combination treatment on T cells activation, TNF-α, IFN-γ and IL-6 were detected from the co-culture medium with ELISA assay. The data showed the TNF-α, IFN-γ and IL-6 were significantly increased in co-culture medium treated by PD0325901 plus PD-1 antibody treatment compared to PD0325901 or PD-1 antibody alone (Fig. 3A). Similarly, there was a significant increase of TNF-α, IFN-γ and IL-6 released from PBMCs co-cultured with *ERK1*- or *ERK2*-knockdown cells in the presence of PD-1 antibody (Fig. 3B and C).

To further determine if ERK inhibition altered the features of tumor microenvironment, the $CD3^+$ and $granzyme^+$ T cells were detected by immunohistochemistry analysis in mice tumor tissues. A significant increase of $CD3^+$ tumor infiltrating lymphocytes (TILs) was observed in tumor tissues treated with the combination of PD-1 antibody and PD0325901 compared to that of PD-1 antibody or PD0325901 alone (Fig. 3D). The fraction of

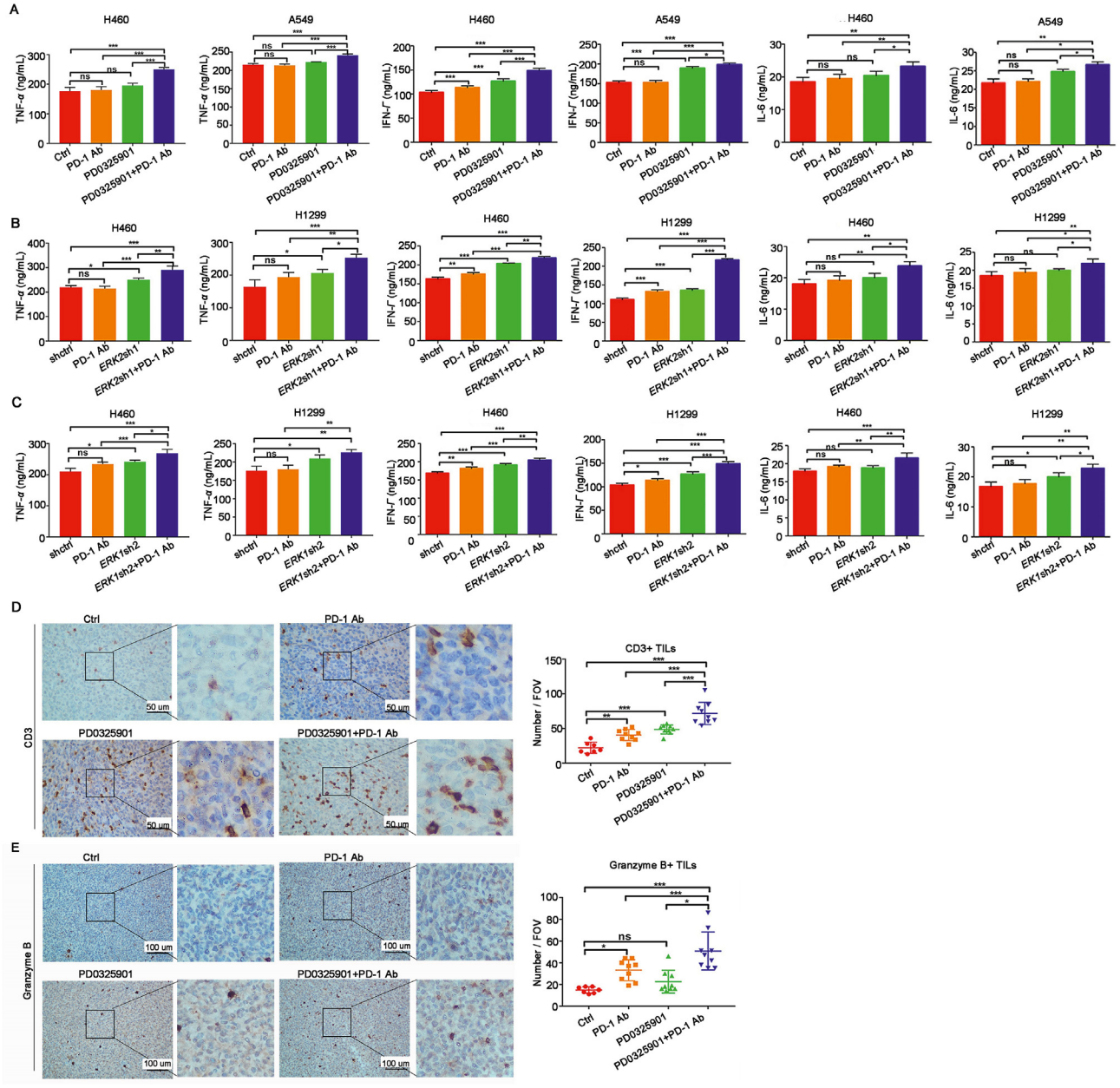

Figure 3 PD0325901 increased lymphocytes infiltration and function. (A) The amounts of TNF-α, IFN-γ, IL-6 from co-culture medium were detected by ELISA assay. (B) and (C) The ELISA assay of TNF-α, IFN-γ, IL-6 from *ERK2*- or *ERK1*-knockdown cells and PBMCs co-culture system. Results are presented as mean ± SD of a representative experiment performed in triplicate. $^*P < 0.05$, $^{**}P < 0.01$, $^{***}P < 0.001$, ns, no significance. (D) and (E) The immunohistochemistry analysis of tumor-infiltrating lymphocytes marker CD3 and granzyme B in tumor tissues isolated from C57BL/6 mice (Ctrl, $n = 7$, others, $n = 9$). The $CD3^+$ T cells were counted at 400× field of view (FOV), and the granzyme B^+ T cells were counted at 200× field of view. Results are presented as mean ± SD; $^*P < 0.05$, $^{**}P < 0.01$, $^{***}P < 0.001$, ns, no significance.

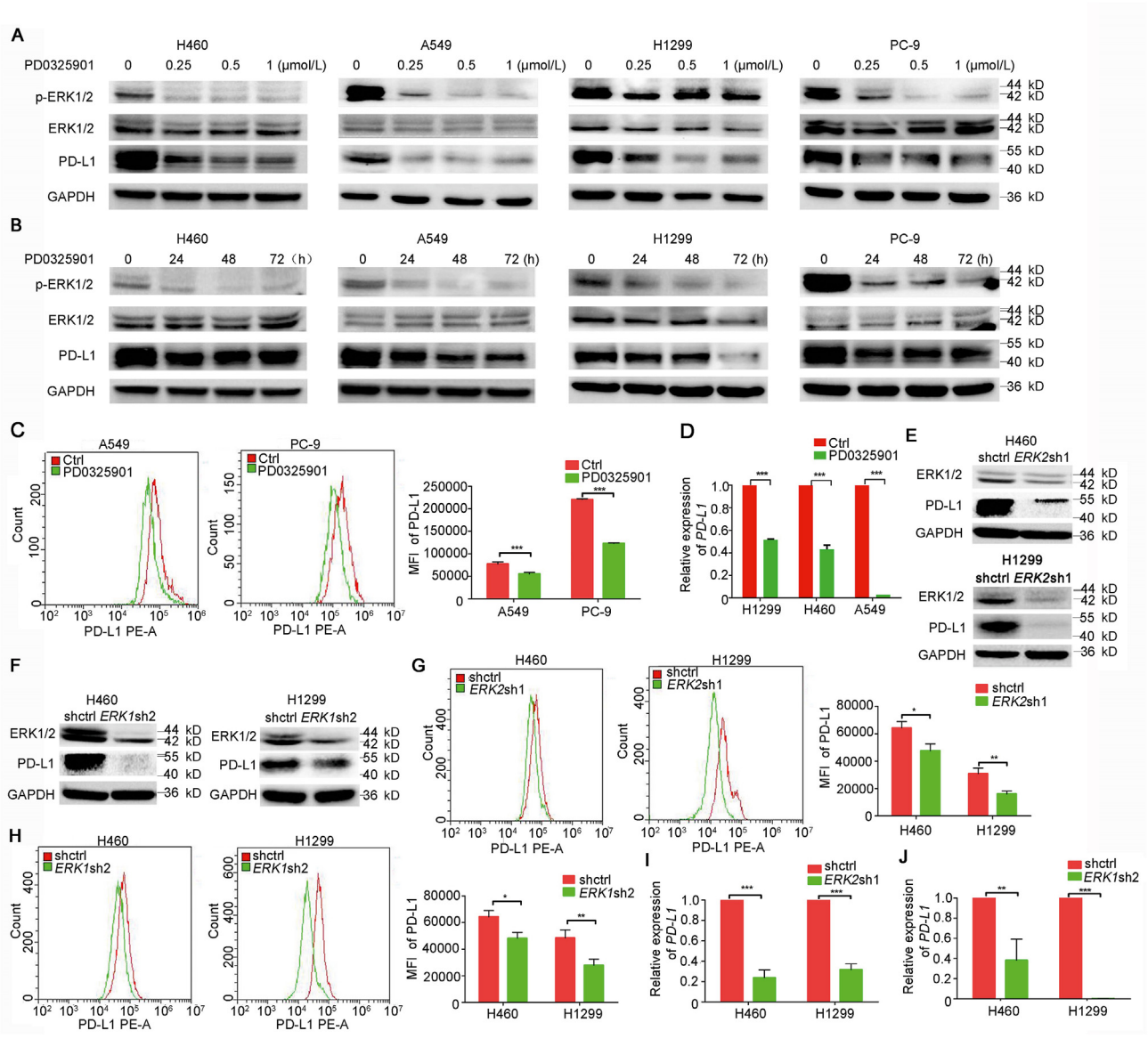

Figure 4 PD0325901 suppressed the PD-L1 expression in NSCLC cells. (A) The Western blotting analysis of PD-L1 expression in NSCLC cells treated with different concentrations of PD0325901 for 48 h. (B) The PD-L1 expression of NSCLC cells treated with PD0325901 at 1 μmol/L for different durations. (C) / analysis of cell membranous PD-L1 expression of NSCLC cells after 1 μmol/L PD0325901 treatment for 48 h. (D) The mRNA level of *PD-L1* detected by quantitative PCR after 1 μmol/L PD0325901 treatment for 48 h. Results are presented as mean ± SD and the experiment was performed in triplicate. $*P < 0.05$, $**P < 0.01$, $***P < 0.001$, ns, no significance. (E) Western blotting analysis of PD-L1 expression in *ERK2*-knockdown cells. (F) Western blotting analysis of PD-L1 expression in *ERK1*-knockdown cells. (G) and (H) The cell membranous PD-L1 expression of *ERK2*- or *ERK1*-knockdown cells. (I) and (J) The mRNA level of *PD-L1* in *EKR1/2*-knockdown cells. Results are presented as mean ± SD of a representative experiment performed in triplicate; $*P < 0.05$, $**P < 0.01$, $***P < 0.001$, ns, no significance.

granzyme B^+ lymphocytes was also increased in the combination treatment group relative to monotherapy groups (Fig. 3E). Together, these data suggest that ERK1/2 inhibition by PD0325901 not only increases lymphocyte cell infiltration, but also enhances the function of lymphocytes as well.

3.6. PD0325901 suppressed PD-L1 expression in NSCLC cells

To explore the effect of blocking ERK activation with PD0325902 on PD-L1 expression, the Western blotting was used to detect the PD-L1 expression in NSCLC cells treated with PD0325901 of different concentrations and durations. The results showed that the PD0325901 was capable of suppressing ERK1/2 activation and inhibiting the PD-L1 expression in concentration- and time-dependent manner in various NSCLC cells (Fig. 4A and B). The PD-L1 expression on cell membranes was also decreased after PD0325901 (1 μmol/L, 48 h) treatment as detected by flow cytometry analysis (Fig. 4C). To identify the mechanism of PD-L1 expression downregulated by PD0325901, the mRNA level of *PD-L1* expression of NSCLC cells was detected by qPCR. The results showed the *PD-L1* mRNA level was significantly decreased by PD0325901 treatment (1 μmol/L,

48 h; Fig. 4D). Likewise, there were notable decreases of PD-L1 expression in *ERK1*- and *ERK2*-knowdown NSCLC cells, respectively (Fig. 4E and F). The PD-L1 expression on cell surface was also decreased in *ERK1*- and *ERK2*-knockdown cells, respectively (Fig. 5G and H). The mRNA expression level of *PD-L1* gene was lower in *ERK1*- or *ERK2*-knockdown cells than that in control cells (Fig. 4I and J).

3.7. *The PD-L1 expression was positively correlated with ERK1/2 phosphorylation in NSCLC cells*

Next, we explored the correlation of p-ERK1/2 and PD-L1, the p-ERK1/2, ERK1/2 and PD-L1 expression of representative NSCLC cells ($n = 6$) by Western blotting (Fig. 5A). The results showed the p-ERK1/2 and PD-L1 expression was positively correlated (Fig. 5B). To further confirm the result, 29 NSCLC patients' tumor tissues from Sun Yat-sen University Cancer Center were collected, and the expressions of PD-L1 and p-ERK1/2 in tumor tissues were analyzed by immunohistochemistry (Fig. 5C and D). The patients with high p-ERK1/2 activation were observed with PD-L1 overexpression (Fig. 5E), and there was a positive correlation between PD-L1 and p-ERK1/2 activation in NSCLC tumor samples (Fig. 5F).

3.8. *Patients who responded to PD-1/PD-L1 inhibitor treatment has low p-ERK activation and abundant infiltrating T cells*

To further validate the antitumor effect of p-ERK inhibition in combination with PD-1 inhibitor, 37 pathological tissue samples of advanced NSCLC patients treated with PD-1/PD-L1 inhibitors were analyzed by immunohistochemistry. The clinical data was collected from pathology reports and medical files. The response to PD-1/PD-L1 inhibitors was assessed according to the immune RECIST (iRECIST)[47]. Of the 37 patients received PD-1/PD-L1 inhibitors therapy, 60% (22/37) patients received pembrolizumab therapy, 32% (12/37) patients were treated with SHR-1210, 5%

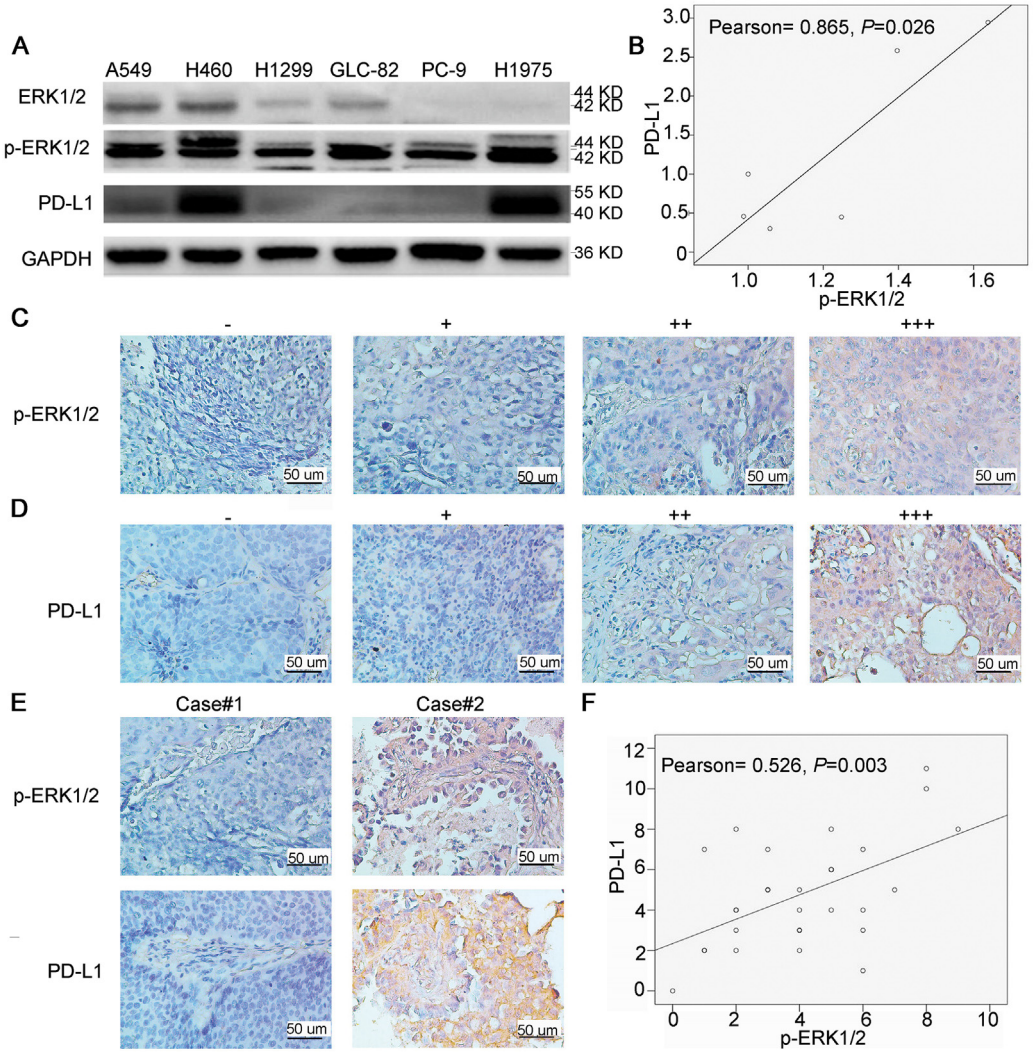

Figure 5 The PD-L1 expression and p-ERK1/2 activation was positively correlated. (A) The Western blotting analysis of the expression of PD-L1, ERK1/2 and p-ERK1/2 in representative NSCLC cells. (B) The Pearson correlation analysis of PD-L1 expression and p-ERK1/2 activation ($n = 6$). (C) The representative pictures of different intensities of p-ERK1/2 activation and (D) PD-L1 expression, the samples were not matched. (E) The PD-L1 expression of NSCLC patients with high or low p-ERK1/2 activation. (F) The Pearson correlation analysis of PD-L1 expression and p-ERK1/2 activation in 29 NSCLC patients.

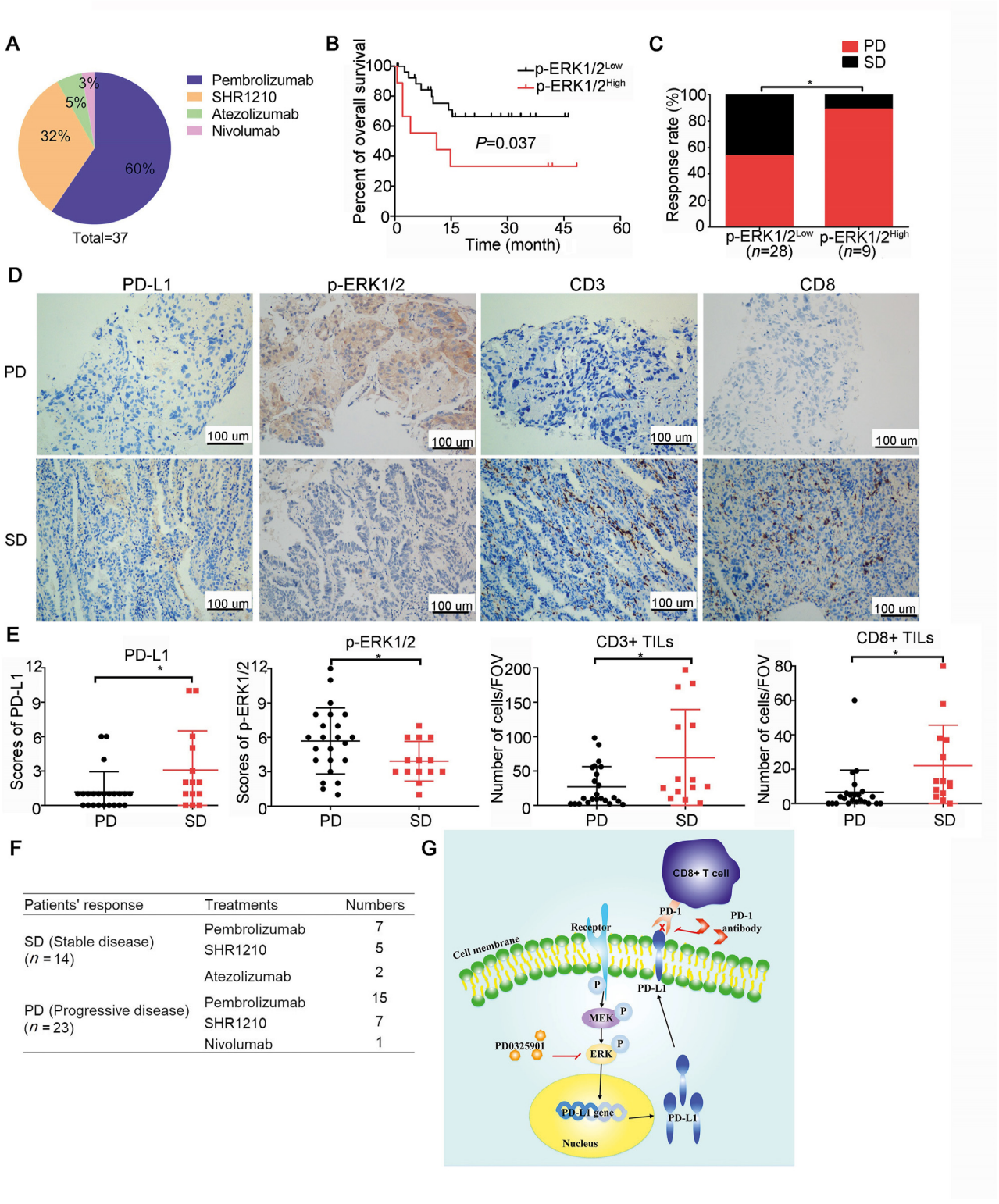

Patients' response	Treatments	Numbers
SD (Stable disease) (n = 14)	Pembrolizumab	7
	SHR1210	5
	Atezolizumab	2
PD (Progressive disease) (n = 23)	Pembrolizumab	15
	SHR1210	7
	Nivolumab	1

Figure 6 Patients who responded to PD-1/PD-L1 inhibitors presented low p-ERK activation and abundant infiltrating lymphocytes. (A) The various treatments of the enrolled 37 NSCLC patients received. (B) The overall survival of patients with high or low p-ERK1/2 activation. The expression of p-ERK1/2 was evaluated by H-score and H-score>8 was considered as high p-ERK1/2 expression, and H-score≤8 was considered as low p-ERK1/2 expression. (C) The response rate of patients with high or low p-ERK1/2 activation. (D) The representative pictures of the expression of different markers in tumor tissues from NSCLC patients who obtained stable disease (SD) or progressive disease (PD) from PD-1/PD-L1 inhibitor therapy. (E) The static analysis of different markers between SD and PD groups. The $CD3^+$ and $CD8^+$ T cells were counted at 200× field of view (FOV). Data are presented as mean ± SD; $^*P < 0.05$, $^{**}P < 0.01$, $^{***}P < 0.001$, ns, no significance. (F) The distribution of the different responses in patients treated with PD-1/PD-L1 inhibitors. (G) A schematic diagram of the mechanism of the combination therapy. PD0325901 suppresses the phosphorylation of ERK1/2 thus decreases the PD-L1 expression on tumor cell membranes, which induces lymphocytes infiltration and activation.

(2/37) patients were administrated with atezolizumab, and 3% (1/37) was nivolumab users (Fig. 6A). The patients with high p-ERK1/2 activation were observed with poor overall survival and high response rate of progressive disease compared to those with low p-ERK1/2 activation (Fig. 6B and C). The patients who got stable disease were observed with high PD-L1 expression compared to those developed progressive disease (Fig. 6D and E). There was a lower activation of p-ERK1/2 and more tumor infiltrating $CD3^+$ and $CD8^+$ T cells in tumor tissue of patients with stable disease than that in patients with progressive disease (Fig. 6D and E). Of the 37 patients treated with PD-1/PD-L1 antibodies, 14 patients obtained tumor control with stable disease, and the other 23 patients developed progressive disease. The distribution of patients with different responses to PD-1/PD-L1 antibodies is shown in Fig. 6F. A schematic diagram of the mechanism of ERK blockers combining with PD-1 inhibitor was presented in Fig. 6G.

4. Discussion

Cancer immunotherapies, such as those targeting the immune checkpoint, have shown robust responses in various malignancies[48]. Immune checkpoint inhibitors, such as PD-1 antibody, binds to the PD-1 expressed on T cells, and thereby stimulate their proliferative capacity, enabling the immune system to resume its ability to recognize, attack, and destroy cancer cells[49]. However, only a subset of patients responded to PD-1/PD-L1 inhibitor therapy[50]. Immune checkpoint blockade combining with other therapeutic modalities such as targeted therapy is one of the approaches to improve the efficacy of PD-1/PD-L1 antibody in treating cancers. Targeted therapies could induce deep responses in NSCLC patients by blocking actionable mutations that are essential for tumor cell growth and progression[21,22]. Interestingly, patients carried driver mutations in NSCLC cells like *EGFR*, *ALK*, and *KRAS* show limited benefits from immunotherapy, suggests that these oncogenes induce changes in the tumor microenvironment to escape from tumor immuno-surveillance[51,52]. As a result, significant efforts are ongoing to identify and develop combinations that could harness the non-overlapping mechanisms of action of targeted agents and immunotherapy to broaden and increase the durability of responses in clinic.

ERK exerts its activity primarily through the MAPK, mTOR/AKT, and JAK/STAT signaling pathways, which are also involved in the regulation of PD-L1 expression[24,25,53]. The PD-L1 expression in tumor cells is associated with poor overall survival[11]. Therefore, it is conceivable that PD0325901 could have an impact on PD-L1 expression in tumor cells and thus enhanced the efficacy of the PD-1 antibody on tumor growth. Consistent with this hypothesis, significant concentration- and time-dependent decreases of PD-L1 expression were observed in NSCLC cells upon PD0325901 treatment. The PD0325901 treatment mediated PD-L1 downregulation on cell membranes in tumor cells. Further analysis showed that ERK inhibitor inhibited the ERK activation, resulting in the reduction of *PD-L1* mRNA level in NSCLC cells. The PD0325901-mediated modulation of PD-L1 expression correlated with the blockade of ERK activation, as demonstrated by the decreases of p-ERK, suggesting that the simultaneous blockade of several ERK downstream pathways might be required to achieve the full magnitude of PD-L1 expression modulation. Downregulation of *ERK1/2 via* shRNAs also led to the downregulation of PD-L1 protein and mRNA levels. These findings implied that activated ERK1/2 signaling pathway was required and sufficient for tumor cells to potentially evade the immune system through the upregulation of PD-L1 expression. The ERK1/2 signaling pathway has been shown to regulate PD-L1 expression in various tumor models[54,55], PD-L1 is transcribed in response to the activation of multiple signaling pathways, and some transcription factors, such as HIF1-α, Myc, STATs, c-JUN and AP-1, have been reported to bind and transactivate *PD-L1* gene[56–59]. Further supporting this idea, the PD-L1 expressions in the NSCLC cells and tumor specimens were positive correlated with the p-ERK activation, respectively. Downregulation of PD-L1 expression in tumor cells was consistent with a shift towards a less immunosuppressive tumor microenvironment that was more permissive to T cells infiltration, because the PD-L1 expression on either tumor cells or host immune cells could lead to tumor escape from immune control[60]. We also tested whether PD0325901 affected the activity of PD-1 antibody *in vitro*. In the co-culture system, the combination treatment of PD0325901 with PD-1 antibody caused more tumor cell lysis than that treated with PD-1 antibody alone. PD0325901-treated tumors exhibited lower PD-L1 expression which could attract more T-cell infiltration[60]. There were significant increases of TNF-α, IFN-γ and IL-6 (T-cell activation marker) secretion in the co-culture system treated with combination treatment compared to PD-1 antibody or PD0325901 alone. A similar result was observed in PBMCs co-culturing with *ERK1*- or *ERK2*-knockdown cells treated by PD-1 antibody, suggesting that inhibition of ERK1/2 pathway would create a more inflamed tumor favorable to be identified and killed by lymphocytes. Previous studies proved that blockade of the ERK phosphorylation could increase the constitutive expression of MHC-I[31], and reduce the apoptosis of T cells and increase the production of cytokines associated with lymphocyte activation[61].

In animal study, there was no significant difference between control and PD0325901 treatment in tumor growth inhibition in NSG mice, but the tumor volumes were obviously decreased in PD0325901 treatment alone in immune-competent C57BL/6 mice, suggesting that the combination treatment in C57BL/6 mice was a result of enhanced immune clearance. The treatment with anti-mouse PD-1 monotherapy resulted in obvious tumor control, or survival benefit, but the effect was not nearly as effective as the combined group, suggesting that there might be other mechanisms of resistance. Primary resistance to PD-1 blockade may be a consequence of ERK alterations in tumor cells driving an immune-suppressive tumor microenvironment. Consistently, the combination with PD0325901 overcame the immunosuppressive microenvironment, allowing for T-cell infiltration and specific antitumor responses which led to a significant survival advantage in mice model. The enhanced survival benefit by combination treatment could also be attributed to a more complete shutdown of the PD-1/PD-L1 axis *via* PD0325901-mediated inhibition of PD-L1 expression in tumor cells and PD-1 antibody mediated blockade of PD-1 in host immune cells. PD-1 antibody in combination with PD0325901 led to additional changes in the immune tumor microenvironment, including increased $CD3^+$ T cells abundance, and a higher proliferative, activated state of granzyme B^+ T cells relative to PD-1 antibody alone as assessed by immunohistochemistry analysis. High tumor-infiltrating lymphocytes' presence was associated with superior prognosis in multiple solid tumors[13,60]. Lack of response to immunotherapy was characterized by several factors, such as a non-inflamed tumor

microenvironment with limited infiltrating T cells and/or the presence of immunosuppressive cell types. It is conceivable that the survival benefit observed in the combination-treated mice could result from the PD-1 antibody mediated enhancement of antitumor responses primed by PD0325901 induced cell killing. A trend of increased T cell infiltration may be essential in the combination-treated mice to trigger deeper antitumor responses, especially in the context of cancers with limited tumor antigens. The shift in the microenvironment of combination-treated tumors towards a more productive inflammatory milieu likely supports and/or enhances antitumor immune responses. Consistent with these data, it has been shown that direct killing of tumor cells with targeted agents such as BRAF and MEK inhibitors cause immunogenic cell death and enhance immunogenicity by driving re-expression of tumor antigens and T-cell infiltration, ultimately leading to increased sensitivity to checkpoint blockade[29,62]. In our study, the patients with high p-ERK activation were associated with poor survival and high response rate of progressive disease after PD-1/PD-L1 antibody treatment. The patients who obtained stable disease rather than progressive disease from PD-1/PD-L1 inhibitors presented low p-ERK activation and abundant $CD3^+$ and $CD8^+$ T cells infiltration. These data pointed out that the activation of the ERK pathway was associated with non-T cell-inflamed tumors resistant to checkpoint blockade, suggesting that the inhibition of ERK activation may be employed as a way to elicit T-cell infiltration. Moreover, the patients with stable disease have higher PD-L1 expression in tumor tissue than that of patients who got progressive disease, as previously reported, the patients with positive high PD-L1 expression presented better responses to PD-1/PD-L1 blockage therapy[63]. Limited studies to date have studied the effect of ERK pathway modulation on the immune subsets. Preclinical and clinical evidences showed that the ERK activation activated by EGFR signaling inhibited the activity of cytotoxic T cells and reduced the number of tumor infiltrating $CD8^+$ lymphocytes[64,65]. More importantly, inhibiting the EGFR/MEK/ERK pathway by EGFR-tyrosine kinase inhibitors could reduce the apoptosis of T cells and increase the production of IFN-γ[61]. Therefore, the mechanisms through which ERK inhibition alone or in combination with PD-1 blockade alter specific immune subsets in the tumor microenvironment such as tumor associated macrophages, dendritic cells, NK and B cells remain to be explored further.

5. Conclusions

We demonstrate that the PD0325901, an ERK1/2 small molecule inhibitor, enhances the efficacy of PD-1 blockade on the inhibition of tumor growth *in vivo* and *in vitro*. Our study shows that PD0325901 treatment could drive T-cell infiltration and activation that was likely critical to induce productive antitumor immune responses. These data provide a rationale for the clinical evaluation of PD0325901 in combination with PD-1/PD-L1 blocking agents in the treatment of NSCLC.

Availability of data and materials

All data generated or analyzed during this study are included in this published article. And the raw data was deposited onto the Research Data Deposit public platform (www.researchdata.org.cn), with the approval RDD number as RDDB2021001035.

Acknowledgments

We thank the grants from the National Science & Technology Major Project "Key New Drug Creation and Manufacturing Program", China (No: 2018ZX09711002), the National Natural Science Foundation of China (No: 81673463).

Author contributions

Min Luo: conceptualization, methodology, validation, formal analysis, investigation, writing-original draft, writing-review & editing, visualization. Yuhui Xia: methodology, validation, investigation. Fang Wang: writing-review & editing, visualization. Hong Zhang: methodology, writing-review & editing. Danting Su: methodology, validation, investigation. Chaoyue Su: investigation. Chuan Yang: investigation. Shaocong Wu: writing-review & editing. Sainan An: writing-review & editing. Suxia Lin: resources, supervision, project administration. Liwu Fu: conceptualization, supervision, project administration, funding acquisition, writing-review & editing.

Conflicts of interest

The authors declare no conflicts of interest.

References

1. Siegel RL, Miller KD, Jemal A. Cancer statistics, 2018. *CA Cancer J Clin* 2018;**68**:7−30.
2. Zappa C, Mousa SA. Non-small cell lung cancer: current treatment and future advances. *Transl Lung Cancer Res* 2016;**5**:288−300.
3. Molina JR, Yang P, Cassivi SD, Schild SE, Adjei AA. Non-small cell lung cancer: epidemiology, risk factors, treatment, and survivorship. *Mayo Clin Proc* 2008;**83**:584−94.
4. Malhotra J, Jabbour SK, Aisner J. Current state of immunotherapy for non-small cell lung cancer. *Transl Lung Cancer Res* 2017;**6**:196−211.
5. Torre LA, Bray F, Siegel RL, Ferlay J, Lortet-Tieulent J, Jemal A. Global cancer statistics, 2012. *CA Cancer J Clin* 2015;**65**:87−108.
6. Wang C, Yu X, Wang W. A meta-analysis of efficacy and safety of antibodies targeting PD-1/PD-L1 in treatment of advanced nonsmall cell lung cancer. *Medicine* 2016;**95**:e5539.
7. Topalian SL, Drake CG, Pardoll DM. Immune checkpoint blockade: a common denominator approach to cancer therapy. *Cancer Cell* 2015;**27**:450−61.
8. Lee CK, Man J, Lord S, Cooper W, Links M, Gebski V, et al. Clinical and molecular characteristics associated with survival among patients treated with checkpoint inhibitors for advanced non-small cell lung carcinoma a systematic review and meta-analysis. *JAMA Oncol* 2018;**4**:210−6.
9. Quezada SA, Peggs KS, Simpson TR, Allison JP. Shifting the equilibrium in cancer immunoediting: from tumor tolerance to eradication. *Immunol Rev* 2011;**241**:104−18.
10. Zerdes I, Matikas A, Bergh J, Rassidakis GZ, Foukakis T. Genetic, transcriptional and post-translational regulation of the programmed death protein ligand 1 in cancer: biology and clinical correlations. *Oncogene* 2018;**37**:4639−61.
11. Ma G, Deng Y, Jiang H, Li W, Wu Q, Zhou Q. The prognostic role of programmed cell death-ligand 1 expression in non-small cell lung cancer patients: an updated meta-analysis. *Clin Chim Acta* 2018;**482**:101−7.
12. Dong H, Strome SE, Salomao DR, Tamura H, Hirano F, Flies DB, et al. Tumor-associated B7-H1 promotes T-cell apoptosis: a potential mechanism of immune evasion. *Nat Med* 2002;**8**:793−800.

13. Shien K, Papadimitrakopoulou VA, Wistuba II . Predictive biomarkers of response to PD-1/PD-L1 immune checkpoint inhibitors in non-small cell lung cancer. *Lung Cancer* 2016;**99**:79−87.
14. Lu W, Lu L, Feng Y, Chen J, Li Y, Kong X, et al. Inflammation promotes oral squamous carcinoma immune evasion *via* induced programmed death ligand-1 surface expression. *Oncol Lett* 2013;**5**:1519−26.
15. Wang J, Chmielowski B, Pellissier J, Xu R, Stevinson K, Liu FX. Cost-effectiveness of pembrolizumab *versus* ipilimumab in ipilimumab-naive patients with advanced melanoma in the United States. *J Manag Care Spec Pharm* 2017;**23**:184−94.
16. Robert C, Ribas A, Schachter J, Arance A, Grob JJ, Mortier L, et al. Pembrolizumab *versus* ipilimumab in advanced melanoma (KEYNOTE-006): *post-hoc* 5-year results from an open-label, multicentre, randomised, controlled, phase 3 study. *Lancet Oncol* 2019;**20**:1239−51.
17. Palakurthi S, Kuraguchi M, Zacharek SJ, Zudaire E, Huang W, Bonal DM, et al. The combined effect of FGFR inhibition and PD-1 blockade promotes tumor-intrinsic induction of antitumor immunity. *Cancer Immunol Res* 2019;**7**:1457−71.
18. Formenti SC, Demaria S. Combining radiotherapy and cancer immunotherapy: a paradigm shift. *J Natl Cancer Inst* 2013;**105**:256−65.
19. Insinga RP, Vanness DJ, Feliciano JL, Vandormael K, Traore S, Ejzykowicz F, et al. Cost-effectiveness of pembrolizumab in combination with chemotherapy *versus* chemotherapy and pembrolizumab monotherapy in the first-line treatment of squamous non-small-cell lung cancer in the US. *Curr Med Res Opin* 2019;**35**:1241−56.
20. Shaw AT, Ou SHI, Bang YJ, Camidge DR, Solomon BJ, Salgia R, et al. Crizotinib in ROS1-rearranged non-small-cell lung cancer. *N Engl J Med* 2014;**371**:1963−71.
21. Zhou CC, Wu YL, Chen GY, Feng JF, Liu XQ, Wang CL, et al. Erlotinib *versus* chemotherapy as first-line treatment for patients with advanced EGFR mutation-positive non-small-cell lung cancer (OPTIMAL, CTONG-0802): a multicentre, open-label, randomised, phase 3 study. *Lancet Oncol* 2011;**12**:735−42.
22. Solomon BJ, Mok T, Kim DW, Wu YL, Nakagawa K, Mekhail T, et al. First-line crizotinib versus chemotherapy in ALK-positive lung cancer. *N Engl J Med* 2014;**371**:2167−77.
23. Bivona TG, Doebele RC. A framework for understanding and targeting residual disease in oncogene-driven solid cancers. *Nat Med* 2016;**22**:472−8.
24. Sumimoto H, Imabayashi F, Iwata T, Kawakami Y. The BRAF-MAPK signaling pathway is essential for cancer-immune evasion in human melanoma cells. *J Exp Med* 2006;**203**:1651−6.
25. Lastwika KJ, Wilson 3rd W, Li QK, Norris J, Xu H, Ghazarian SR, et al. Control of PD-L1 expression by oncogenic activation of the AKT-mTOR pathway in non-small cell lung cancer. *Cancer Res* 2016;**76**:227−38.
26. Akbay EA, Koyama S, Carretero J, Altabef A, Tchaicha JH, Christensen CL, et al. Activation of the PD-1 pathway contributes to immune escape in EGFR-driven lung tumors. *Cancer Discov* 2013;**3**:1355−63.
27. Azuma K, Ota K, Kawahara A, Hattori S, Iwama E, Harada T, et al. Association of PD-L1 overexpression with activating EGFR mutations in surgically resected nonsmall-cell lung cancer. *Ann Oncol* 2014;**25**:1935−40.
28. Chen DS, Mellman I. Oncology meets immunology: the cancer-immunity cycle. *Immunity* 2013;**39**:1−10.
29. Frederick DT, Piris A, Cogdill AP, Cooper ZA, Lezcano C, Ferrone CR, et al. BRAF inhibition is associated with enhanced melanoma antigen expression and a more favorable tumor microenvironment in patients with metastatic melanoma. *Clin Cancer Res* 2013;**19**:1225−31.
30. Knight DA, Ngiow SF, Li M, Parmenter T, Mok S, Cass A, et al. Host immunity contributes to the anti-melanoma activity of BRAF inhibitors. *J Clin Invest* 2013;**123**:1371−81.
31. Pollack BP, Sapkota B, Cartee TV. Epidermal growth factor receptor inhibition augments the expression of MHC class I and II genes. *Clin Cancer Res* 2011;**17**:4400−13.
32. Mascia F, Schloemann DT, Cataisson C, McKinnon KM, Krymskaya L, Wolcott KM, et al. Cell autonomous or systemic EGFR blockade alters the immune-environment in squamous cell carcinomas. *Int J Cancer* 2016;**139**:2593−7.
33. Zassadowski F, Rochette-Egly C, Chomienne C, Cassinat B. Regulation of the transcriptional activity of nuclear receptors by the MEK/ERK1/2 pathway. *Cell Signal* 2012;**24**:2369−77.
34. Balmanno K, Cook SJ. Tumour cell survival signalling by the ERK1/2 pathway. *Cell Death Differ* 2009;**16**:368−77.
35. See WL, Tan IL, Mukherjee J, Nicolaides T, Pieper RO. Sensitivity of glioblastomas to clinically available MEK inhibitors is defined by neurofibromin 1 deficiency. *Cancer Res* 2012;**72**:3350−9.
36. Haura EB, Ricart AD, Larson TG, Stella PJ, Bazhenova L, Miller VA, et al. A phase II study of PD-0325901, an oral MEK inhibitor, in previously treated patients with advanced non-small cell lung cancer. *Clin Cancer Res* 2010;**16**:2450−7.
37. LoRusso PM, Krishnamurthi SS, Rinehart JJ, Nabell LM, Malburg L, Chapman PB, et al. Phase I pharmacokinetic and pharmacodynamic study of the oral MAPK/ERK kinase inhibitor PD-0325901 in patients with advanced cancers. *Clin Cancer Res* 2010;**16**:1924−37.
38. Zhang Z, Guo X, To KKW, Chen Z, Fang X, Luo M, et al. Olmutinib (HM61713) reversed multidrug resistance by inhibiting the activity of ATP-binding cassette subfamily G member 2 *in vitro* and *in vivo*. *Acta Pharm Sin B* 2018;**8**:563−74.
39. Zhang H, Huang L, Tao L, Zhang J, Wang F, Zhang X, et al. Secalonic acid D induces cell apoptosis in both sensitive and ABCG2-overexpressing multidrug resistant cancer cells through upregulating c-Jun expression. *Acta Pharm Sin B* 2019;**9**:516−25.
40. Xu M, Wang F, Li G, Wang X, Fang X, Jin H, et al. MED12 exerts an emerging role in actin-mediated cytokinesis *via* LIMK2/cofilin pathway in NSCLC. *Mol Cancer* 2019;**18**:93.
41. Li CW, Lim SO, Xia W, Lee HH, Chan LC, Kuo CW, et al. Glycosylation and stabilization of programmed death ligand-1 suppresses T-cell activity. *Nat Commun* 2016;**7**:12632.
42. Luo F, Luo M, Rong QX, Zhang H, Chen Z, Wang F, et al. Niclosamide, an antihelmintic drug, enhances efficacy of PD-1/PD-L1 immune checkpoint blockade in non-small cell lung cancer. *J Immunother Cancer* 2019;**7**:245.
43. Dorand RD, Nthale J, Myers JT, Barkauskas DS, Avril S, Chirieleison SM, et al. Cdk5 disruption attenuates tumor PD-L1 expression and promotes antitumor immunity. *Science* 2016;**353**:399−403.
44. Carnevalli LS, Sinclair C, Taylor MA, Gutierrez PM, Langdon S, Coenen-Stass AML, et al. PI3Kalpha/delta inhibition promotes anti-tumor immunity through direct enhancement of effector $CD8^+$ T-cell activity. *J Immunother Cancer* 2018;**6**:158.
45. Babon JA, DeNicola ME, Blodgett DM, Crèvecoeur I, Buttrick TS, Maehr R, et al. Analysis of self-antigen specificity of islet-infiltrating T cells from human donors with type 1 diabetes. *Nat Med* 2016;**22**:1482−7.
46. Malekzadeh P, Pasetto A, Robbins PF, Parkhurst MR, Paria BC, Jia L, et al. Neoantigen screening identifies broad TP53 mutant immunogenicity in patients with epithelial cancers. *J Clin Invest* 2019;**129**:1109−14.
47. Seymour L, Bogaerts J, Perrone A, Ford R, Schwartz LH, Mandrekar S, et al. iRECIST: guidelines for response criteria for use in trials testing immunotherapeutics. *Lancet Oncol* 2017;**18**:e143−52.
48. Zhao J, Xiao ZL, Li TT, Chen HQ, Yuan Y, Wang YA, et al. Stromal modulation reverses primary resistance to immune checkpoint blockade in pancreatic cancer. *ACS Nano* 2018;**12**:9881−93.
49. Zhao M, Guo W, Xu Q, Sun Y. SHP2 inhibition triggers anti-tumor immunity and synergizes with PD-1 blockade. *Acta Pharm Sin B* 2019;**9**:304−15.
50. Pardoll DM. The blockade of immune checkpoints in cancer immunotherapy. *Nat Rev Cancer* 2012;**12**:252−64.

51. Martin-Orozco E, Sanchez-Fernandez A, Ortiz-Parra I, Ayala-San Nicolas M. WNT signaling in tumors: the way to evade drugs and immunity. *Front Immunol* 2019;**10**:2854.
52. Ho PC, Meeth KM, Tsui YC, Srivastava B, Bosenberg MW, Kaech SM. Immune-based antitumor effects of BRAF inhibitors rely on signaling by CD40L and IFNgamma. *Cancer Res* 2014;**74**: 3205−17.
53. Abdelhamed S, Ogura K, Yokoyama S, Saiki I, Hayakawa Y. AKT-STAT3 pathway as a downstream target of EGFR signaling to regulate PD-L1 expression on NSCLC cells. *J Cancer* 2016;**7**:1579−86.
54. Yamamoto R, Nishikori M, Tashima M, Sakai T, Ichinohe T, Takaori-Kondo A, et al. B7-H1 expression is regulated by MEK/ERK signaling pathway in anaplastic large cell lymphoma and Hodgkin lymphoma. *Cancer Sci* 2009;**100**:2093−100.
55. Shi J, Qin X, Zhao L, Wang G, Liu C. Human immunodeficiency virus type 1 Tat induces B7-H1 expression *via* ERK/MAPK signaling pathway. *Cell Immunol* 2011;**271**:280−5.
56. Ginsberg M, Czeko E, Muller P, Ren Z, Chen X, Darnell Jr JE. Amino acid residues required for physical and cooperative transcriptional interaction of STAT3 and AP-1 proteins c-Jun and c-Fos. *Mol Cell Biol* 2007;**27**:6300−8.
57. Green MR, Rodig S, Juszczynski P, Ouyang J, Sinha P, O'Donnell E, et al. Constitutive AP-1 activity and EBV infection induce PD-L1 in Hodgkin lymphomas and posttransplant lymphoproliferative disorders: implications for targeted therapy. *Clin Cancer Res* 2012;**18**:1611−8.
58. Zhang N, Zeng YY, Du WW, Zhu JJ, Shen D, Liu ZY, et al. The EGFR pathway is involved in the regulation of PD-L1 expression *via* the IL-6/JAK/STAT3 signaling pathway in EGFR-mutated non-small cell lung cancer. *Int J Oncol* 2016;**49**:1360−8.
59. Luo M, Wang F, Zhang H, To KKW, Wu S, Chen Z, et al. Mitomycin C enhanced the efficacy of PD-L1 blockade in non-small cell lung cancer. *Signal Transduct Target Ther* 2020;**5**:141.
60. Bence C, Hofman V, Chamorey E, Long-Mira E, Lassalle S, Albertini AF, et al. Association of combined PD-L1 expression and tumour-infiltrating lymphocyte features with survival and treatment outcomes in patients with metastatic melanoma. *J Eur Acad Dermatol Venereol* 2019;**34**:984−94.
61. Chen N, Fang WF, Zhan JH, Hong SD, Tang YN, Kang SY, et al. Upregulation of PD-L1 by EGFR activation mediates the immune escape in EGFR-driven NSCLC implication for optional immune targeted therapy for NSCLC patients with EGFR mutation. *J Thorac Oncol* 2015;**10**:910−23.
62. Liu L, Mayes PA, Eastman S, Shi H, Yadavilli S, Zhang TD, et al. The BRAF and MEK inhibitors dabrafenib and trametinib: effects on immune function and in combination with immunomodulatory antibodies targeting PD-1, PD-L1, and CTLA-4. *Clin Cancer Res* 2015; **21**:1639−51.
63. Taube JM, Klein A, Brahmer JR, Xu H, Pan X, Kim JH, et al. Association of PD-1, PD-1 ligands, and other features of the tumor immune microenvironment with response to anti-PD-1 therapy. *Clin Cancer Res* 2014;**20**:5064−74.
64. Helland A, Brustugun OT, Nakken S, Halvorsen AR, Donnem T, Bremnes R, et al. High number of kinome-mutations in non-small cell lung cancer is associated with reduced immune response and poor relapse-free survival. *Int J Cancer* 2017;**141**:184−90.
65. Busch SE, Hanke ML, Kargl J, Metz HE, MacPherson D, Houghton AM. Lung cancer subtypes generate unique immune responses. *J Immunol* 2016;**197**:4493−503.